Conf-9410131--7
SAND-93-3909C

Computational Design of Hypervelocity Launchers

Timothy Trucano[1] and Lalit Chhabildas[2]

[1]Computational Physics Research and Development Department, 1431

[2]Experimental Impact Physics Department, 1433

Sandia National Laboratories

P. O. Box 5800

Albuquerque, New Mexico 87185

Keywords: Hypervelocity Launcher; Eulerian computational hydrodynamics; CTH; Impact techniques; hypervelocity projectiles

ABSTRACT

The Sandia Hypervelocity Launcher (*HVL*) uses impact techniques on a two-stage light-gas gun to launch flier plates to velocities in excess of 10 km/s. An important problem in designing successful third stage techniques for impact launching fliers to such velocities is detailed understanding of the interior ballistic performance of the third stage. This is crucial for preventing melt and fracture of the flier plates during the extraordinary accelerations that they undergo (accelerations on the order of 10^9 g are typical on the HVL). We seek to optimize HVL launch conditions in order to achieve two major goals: first, to maximize the potential launch velocity for a given flier, and second, to allow different flier configurations. One tool that we can apply in studying HVL performance is the use of multi-dimensional wave propagation codes. We have used such codes, particularly the Sandia Eulerian code **CTH**, to study a variety of interior ballistics issues related to gun performance and launcher development for almost ten years. Recently this work has culminated in a major contribution to HVL design, namely the capability to launch "chunk" fliers. The initial phases of design development were solely devoted to **CTH** computations that studied potential designs, identified problems, and posed possible solutions for launching chunk fliers on the HVL. Our computations sufficiently narrowed the design space to the point that systematic experimental progress was possible. Our first experiment resulted in the successful launch of an intact 0.33 gram titanium alloy chunk flier to a velocity of 10.2 km/s. The thickness to diameter ratio of this flier was approximately 0.5.

This work performed at Sandia National Laboratories supported by the U. S. Department of Energy under contract number DE-AC04-94AL85000.

DISCLAIMER

Portions of this document may be illegible in electronic image products. Images are produced from the best available original document.

1. Introduction

The Sandia HyperVelocity Launcher (*HVL*) (Chhabildas, 1992; Chhabildas, *et al*, 1991; 1992; 1993a) uses a sacrificial third stage barrel, the ***barrel extension***, added to a standard two-stage light gas gun to successfully accelerate flier plates to velocities in excess of 15 km/s (Chhabildas, *et al*, 1994a). The operation of this type of launcher is briefly described as follows: A two-stage light gas gun projectile is launched and strikes the flier within the barrel extension. The nose of the two-stage gun projectile is specially designed to produce an approximately shockless pressure wave exceeding one megabar in magnitude. The barrel extension is designed to prevent decompression of the impact prior to attainment of peak acceleration. The high pressures induce flier accelerations which are on the order of 10^9 g's (1 g = 980 cm/sec^2). Because of the high pressures this fixture is destroyed during an experiment and must be replaced. The flier is thin, typically on the order of 0.5 mm to 1.0 mm in thickness. The flier plate itself consists of a central piece of titanium alloy or other metal, approximately 2 cm in diameter, with a surrounding guard ring of the same metal that isolates the central piece during acceleration. The combined diameter of the central flier plus the guard ring is equal to the diameter of the Sandia two-stage gun barrel, approximately 3 cm. A low density plastic may also be joined to the flier plate on the impact side to provide further impact cushioning. The hypervelocity fliers which result from this technique have been applied to both general phenomenological studies (Chhabildas, *et al*, 1993b) and precision equation of state studies (Brannon and Chhabildas, 1994).

The impactor, the flier plate configuration, and the barrel extension in the HVL must all work synergistically in order to successfully launch the flier to velocities exceeding 10 km/s. The simplest proof of this statement is to note that the world record 15 km/s launch mentioned above (Chhabildas, *et al*, 1994a) occurred using an impactor having a velocity of less than 7 km/s. Thus, the terminal flier velocity well exceeds the theoretical achievable velocity limit of twice the impact velocity for an infinitely massive impactor in planar geometry. Since energy releasing materials (explosives, for example) are not used to produce flier velocity gain in HVL experiments, it is clear that a very complex pattern of momentum transfer from the impactor to the flier takes place in order to produce such high velocities. The critical phenomena that are controlled by the three major components of the HVL (impactor, flier, and barrel extension) are (1) the application of a carefully shaped pressure pulse to accelerate the flier without melting or spall and (2) survival of the flier under the high accelerations (roughly nine orders of magnitude greater than the acceleration of gravity) and residual high pressures.

The impactor design and the use of a low-density cushion on the flier are critical to shaping the loading pressure properly. The current impactor design uses a series of layers that have varying shock impedances. The lowest impedance material is placed at the impact side, with impedance increasing as depth in the impactor increases. (Figure 2 illustrates this in a simple case.) The design principles for graded density impactors are now standard, and have been discussed in previous publications (Barker, 1984; Chhabildas and Barker, 1988; Chhabildas, *et al*, 1988; Chhabildas and Asay, 1992). The key fact for our present discussion is that, aside from fabrication issues, generating a proper loading pulse is primarily a one-dimensional wave propagation problem that is amenable to study with idealized models and one-dimensional shock wave computer codes. The layered impactor design also conveniently scales for varying diameter two-stage gas gun bores, as has been proven by successfully launching HVL fliers on larger bore two-stage guns (Chhabildas, *et al*, 1994).

Achieving a suitable pressure drive is not sufficient to guarantee the success of the HVL, unfortunately. Due to the high pressures and accelerations, tremendous stress gradients may be produced in the flier by its interaction with the surrounding environment. Unless extreme measures are taken to prevent the formation of these gradients, the flier would certainly be mechanically destroyed during launch. As one example, we have found that the flier must be inertially confined by the barrel extension for a precise amount of time during its acceleration. If this time is too short, the decompression of the flier is too rapid and disruption resulting from bending stresses emanating from the initial impact will destroy it. If the confinement time is too long, the "squeezing" of the barrel extension upon the flier will either prevent the flier from achieving a high terminal velocity or will destroy it compressively, or both. Heating of the flier can also increase (paradoxically) if the acceleration is not rapid enough. For the HVL, we have observed that the use of a guard ring in the flier and a high impedance barrel extension basically solve this problem. The magnitude and timing of destructive edge effects is somewhat dependent upon the barrel extension diameter, however, and the rather subtle nature of this dependence must be determined in order to produce a final working design. We refer to this as an ***interior ballistics*** problem for the barrel extension. This is now a multi-dimensional (wave propagation) phenomena.

We have successfully applied two-dimensional shock wave calculations to explore the parameter space determining edge effects in the HVL. Such calculations have helped define the final design of the successful HVL. Multi-dimensional calculations are now sufficiently precise to be relevant for this application with state of the art shock wave physics codes running on current generation computers. We have integrated such calculations into the HVL development program since its inception several years ago. Not only can these calculations reduce the amount of parameter exploration that would otherwise be performed experimentally, but they also provide important analysis of what took place in actual experiments.

A good illustration of the way in which computational analysis is an important component in the HVL development program is the problem of intact launch of a "chunk" flier. These are fliers for which the ***aspect ratio*** - the ratio of flier thickness to flier diameter - is an order of magnitude larger than for the usual HVL fliers, say on the order of 0.5. Thin fliers typically have aspect ratios between 0.1 and 0.05. Chunk fliers are important in phenomenology studies, but have not previously been launched to laboratory velocities in excess of two-stage light gas gun velocities. And, the reader should note that it is not trivial to achieve even these velocities, since special high pressure sabots are required. We seek to launch such fliers to velocities in excess of 10 km/s. No known sabot design can withstand accelerations of 10^9 g's, so new ideas are clearly required to solve this problem.

It turns out that tailoring the pressure drive to prevent chunk flier melting and spall is a straightforward extension of the techniques used for the thin fliers. Thus, the most difficult issue in chunk flier acceleration is related to the interior ballistics. The important scale for the layered impactor generation of a suitable pressure pulse is that of the relative increased thickness of the flier. Increased thickness immediately implies that the layered impactor should also be increased by a similar scale. This is not easy to do because we are constrained by the throw weight of the two-stage gun impactor. To attain nominal impact velocities of 6.0 km/s, the characteristic impact velocity for the thin flier experiments, we must then reduce the diameter of the layered impactor if we increase its thickness at the same time. The differences we have in mind are sketched in Figure 1.

This concept, while natural, now introduces multi-dimensional wave propagation effects into the impact launch of the chunk flier even earlier that for the usual thin HVL flier. The impact conditions are now inhomogeneous in radius, because the graded density layers are no longer as wide as the entire impactor surface. Also, because critical layer thicknesses have increased while the nominal impact pressures are the same, the necessary time for confining the impact increases. An important question is what exactly is a workable barrel extension under these conditions? Answering this question experimentally is non-trivial because of the large parameter space that needs to be explored. The parameters include the geometry and composition of the barrel extension, the composition and size of the flier and its associated guard ring, and special details related to isolating the chunk from the destructive edge effects.

In this paper we summarize part of the computational design analysis that was performed to solve the problem of launching a chunk flier. In Section 2 we will review the **CTH** shock physics code, the computational tool that we apply to the problem. We will then illustrate its use by presenting calculations that lead to the general design of the barrel extension. This discussion will allow the reader to understand how 2-D calculations can be applied for design exploration, thus reducing the amount of experimental effort required to perform a successful launch. The barrel extension concept that is found to work best in the computational exploration uses a reduced diameter, matching the diameter of the chunk to be launched. We refer to this as a ***stepped barrel extension.***

A larger suite of calculations helped refine the experimental design to the point of attempting an experiment. This experiment is described in Section 3. While we would have been quite happy if only a few experiments had been required to achieve a hypervelocity launch for the chunk flier, it turned out that the ***first*** experiment was successful. The terminal velocity of the chunk, 0.33 g of titanium alloy having an aspect ratio of 0.5, was 10.2 km/s.

We will analyze this experiment in some detail in Section 4. This discussion will show the power of computational tools for understanding the details of this complex experiment. Important performance data for experiments on the HVL, such as determination of the interior deformations of the barrel extension, flier, and impactor at peak pressure, have not been measured. This type of diagnostic information can be very difficult to acquire. Computer simulations of the experiments can reveal, with reasonable confidence, qualitative and quantitative behavior of components. Understanding this behavior leads to substantial improvements in HVL launcher performance. Among the observations that follow from the computational analysis of the chunk flier experiment are:

- Two-dimensional effects actually help convert impactor momentum into chunk flier velocity for chunk fliers when the experiment is properly designed.
- The acceleration process for chunk fliers lasts much longer than for thin HVL fliers. It also lasts longer than a purely planar impact geometry in which the various thickness have been uniformly scaled. The lengthened acceleration times demonstrate that the stepped barrel extension exerts a nonlinear effect on the confinement time which is required to achieve peak acceleration for the flier.
- Computations indicate that the flier was close to spalling during its launch. We can further tune the experiment so that a larger safety margin with regard to flier fracture will be present. This will extend our ability for launching fliers of different materials.

We summarize our conclusions in Section 5. We also briefly discuss future directions for research of this type.

2. Computational Exploration of Barrel Extensions

We use the multi-dimensional Eulerian shock wave physics code **CTH** (McGlaun, *et al*, 1990) for our numerical simulations of the HVL. Standard Lagrangian codes can not be applied to this type of analysis because of the large material deformations that take place during peak acceleration in the HVL.

CTH has several features which are important for modeling HVL experiments. These include: (1) **CTH** is a multimaterial code. (2) Materials can be modeled with strength and fracture, and there are a variety of these models presently implemented in the code. (3) High resolution interface tracking and second order accurate numerical algorithms provide a level of accuracy required for precision design analyses. (4) An option is available in **CTH** that allows the user to zero out the rotational components of shear strain in mixed cells which contain an interface between two user specified materials. Technically, this option does not produce a contact surface between these materials similar to that used in Lagrangian codes. It does prevent a type of "sticking" between the materials that is unphysical in sliding dominated contact, such as the interaction between the flier and the guard ring. The user also has the advantage of specifying multiple pairs of materials for which this option is enabled. Our simulations of the HVL (and other gun systems) become highly inaccurate if this option is not used. Its application has been validated versus a variety of experiments and we feel comfortable using it.

For the calculations discussed here, all of the materials were modeled using the ANEOS Mie-Grüneisen equation of state option (Thompson, 1989) and standard material parameters (Hertel, 1992). In the impact region where peak accelerations occur, the mesh resolution was $\Delta r = \Delta z = 0.01$ cm. This implies an axial resolution of thirty zones through the flier. The calculations were performed running **CTH** on HP 735 workstations.

The most important conceptual design issue for accelerating chunk fliers, given that we can generate a proper shockless pressure pulse using a layered impactor, is the nature of the barrel extension. To analyze this problem it is convenient to study a simplified design that still contains the key ingredients of a real experimental configuration. We introduce this simplification by first asking whether we need a special barrel extension at all, or whether the nominal HVL barrel is all that is needed.

The simplification we use is drawn in Figure 2. There, a simplified layered impactor is shown and the corresponding flier plate. In Figure 2 we have shown the nominal HVL barrel configuration with the absence of a step in the barrel. The diameter of the barrel extension is thus the same as that of the two-stage gun used to launch the impactor. The flier thickness and guard ring size have been increased to form a flier that has an aspect ratio of 0.5. The simple four layer impactor has a thickness which has been increased beyond the nominal HVL thicknesses by the same factor as the flier thickness. This idea was suggested in Figure 1. The overall diameter of the metal layers in the impactor has been correspondingly reduced to conform to the two-stage gun throw weight constraint. However, this reduction in diameter of the layers increases the potential for damaging edge effects to ruin the flier acceleration process. The aft part of the lexan impactor body has not been included in this configuration. We assume that the two-stage projectile velocity is always 5.8 km/s, easily achievable on the two-stage gun. The guard ring in Figure 2 is assumed to be constructed of titanium alloy, the same material as the titanium alloy chunk fliers.

Figure 3 shows the **CTH** computed configuration 3.0 μs after impact. We have also shown a plot of the driving pressure resulting from the impact and the axial velocity of the flier, as measured at a point in the middle of the flier. The driving pressure, of course, is quasi-isentropic. This pressure profile would be smoothed by the use of additional layers in the impactor. (An illustration of the smoother profile that was applied in the actual experiment is found in Figure 10). The residual temperatures in the flier are approximately 1000 K, well below the melt temperature of 1900 K for the titanium alloy.

The axial velocity of the flier is also plotted in Figure 3. We see that the flier really did not accelerate beyond the velocity of the impactor. Its terminal velocity was only 6 km/s, essentially the same as the impactor velocity. We also note in the calculation that tensile pressures exceeding 5 GPa formed in the aft part of the flier. Since the dynamic spall strength of the titanium alloy is around 5.5 GPa (Chhabildas, *et al*, 1990a) there is a good possibility that the flier may spall during this launch. This is not visible in the calculated configuration is Figure 3. Our observation of **CTH** simulations of HVL launches has been that the code is a conservative predictor of flier fracture. When **CTH** clearly predicts flier fracture, we typically see that fracture in the corresponding experiment. However, there are cases where the flier may fracture in an experiment and that fracture is not visible in the calculation. This may be partly due to the fact that the simple fracture model in **CTH** allows fractures to "heal" numerically as calculations progress.

One conjecture that follows from this calculation is that a bit more confinement of the flier might increase the peak velocity, at the risk of increasing the resulting tensile stress. The simplest way to increase confinement is to simply change the guard ring to a higher impedance material (think of this as a small "dynamic" gun barrel). We test this idea by performing a calculation with the guard ring composed of the same tungsten alloy as the barrel. The peak velocity of the flier then increases to approximately 7.0 km/s. However, the peak tensile pressures also increase to considerably more that 5 GPa, and the residual temperature of the flier increases to more than 1500 K. This flier will certainly be destroyed by the launch. The confinement is too strong and deforms the flier, as shown in Figure 4, while the achieved velocity is still too low to be of much interest. Release waves from the downstream side of the flier configuration, in particular from the *guard ring*, are prime culprits in the excessive deformation of the flier. The primary problem with these waves is not that they create spall in the flier. Rather, they release the flier from its high pressure state in such a way as to distort and, therefore, create deformation leading to fracture of the flier: This effect also reduces the drive (in other words, momentum transfer from the impactor to the chunk) too early in the impact to achieve really high velocities. The deformation of the flier also contains a component which originated in the multi-dimensional effects generated immediately upon impact. These are caused by the smaller radial extent of the layered materials.

This leads to the next calculation, in which we introduce a stepped barrel extension, also made of tungsten. The initial configuration and the configuration at times 0.0, 1.0, 1.5, and 3.0 μs are shown in Figure 5. By 3.0 μs the flier is almost decoupled from the launch process, although some impactor material jetting down the stepped barrel is clearly visible and provides a small additional increment of flier acceleration. The calculation predicts that this flier will remain intact and not melt.

Figure 6 summarizes the flier axial velocity histories for the three calculations that we have discussed in this section. The velocity with the stepped barrel is 40% higher than a simple un-stepped impact configuration. The two-dimensional effects have significantly contributed to the acceleration of the flier in this case. This is most obvious from

Figure 6 when one examines the overall acceleration time. While the un-stepped calculations have achieved terminal velocity by 2.0 μsec, acceleration continues to take place for the stepped barrel. In fact, the flier is still accelerating slightly even at 3.0 μsec. Note that these acceleration times are nothing like those that we observe for thin fliers on the HVL - there, the acceleration to terminal velocity typically occurs in approximately 1/2 microsecond.

The most important parameters related to the flier in these three calculations have been listed in Table 1. It is interesting that the peak drive pressure experienced by the flier increased by over 25% when we changed from a titanium to a tungsten guard ring. Then, the drive pressure essentially did not change when we used the stepped barrel (still with a tungsten guard ring). We conclude that the driving pressure depends on more than simply the impactor configuration, a severe complication. This idea suggests that confinement of the flier at the right time, and for the right duration, is critical to enhanced acceleration. We also included a column in Table 1 with our appraisal of the state of the flier based on the calculation. With the titanium guard ring, the flier had low temperatures but might fracture. It doesn't matter, though - its velocity is too low to be interesting. With a tungsten guard ring and no stepped barrel, the entire body of the flier went into strong tension; this flier would almost certainly breakup. The flier may not be intact with the stepped barrel, but not because of high tensile stresses. Rather, the temperature of the flier is close to melt. But the velocity is exactly what we want - greater than 10 km/s.

The key features of a successful design seem to be present with our crude stepped barrel design. First, tensile states, while present, are not disastrously large. Second, the edge effects have been controlled so that they do not produce severe bending of the flier, as is clear in Figure 5. Third, the edge effects have served to convert additional impactor momentum into flier acceleration, illustrated by the visible impactor jetting seen in Figure 5 at 3.0 microsecond. Fourth, the impactor was confined for roughly the correct amount of time - a large boost in velocity occurred, due to the push from the jetting impactor materials, but the pressure did not become so large that the flier melted or deformed to the point of destruction. Last, temperatures in the flier can always be lowered by exerting greater care in the design of the impactor.

We could (and originally did) explore variations of the stepped barrel in Figure 5. However, we find that no substantial modification of this concept functions better. Thus, this design served as the focus of an actual experiment. The results of this experiment are discussed in the next section.

3. Experimental Summary

The configuration of the experiment that was performed on the Sandia HVL is shown in Figures 7 and 8. Details of the graded-density impactor and the flier plate configuration are shown in Figure 8. Calculations indicated that the final mechanical state of the flier could be improved if the flier was isolated from the stepped barrel by a guard ring. This was done for the experiment. The titanium alloy flier plate is three times thicker (0.3 cm) than nominal HVL thin fliers (0.1 cm). Because of the presence of the guard ring, the overall diameter of this flier assembly is 1.0 cm. The mass of the central flier is 0.33 g. The central chunk has an aspect ratio of 0.5. A graded-density impactor approximately 3 times the thickness of that used in normal HVL experiments and 1.27 cm in diameter was used. Another difference in the actual experiment from the idealization in Section 2 is that a TPX (a low density hydrocarbon plastic) cushion was

placed flush with the impact side of the flier. A series of calculations was used to refine the proper diameter, thickness, and placement of this TPX cushion.

The layered impactor velocity for the experiment was approximately 5.8 km/s. This velocity was estimated from previous performance data for the two-stage gun, rather than directly measured for this particular experiment. This estimate is accurate to within 2%. Radiographic measurements of the chunk flier and the guard ring are taken along its flight path after exit from the tungsten barrel extension and up to flight distances of over 1.4 meters after impact. Sample radiographs are shown in Figure 9, along with a plot of distance traveled versus time for the radiographs. These data were fit with a linear regression to show that the velocity of the flier for this experiment was 10.2 km/s. The flier is observed to be intact from the radiography. The flier appears to be tumbling as it traverses the target chamber, and has rotated approximately half a turn over the total flight distance. Tumbling is a three-dimensional effect that can not be predicted by two-dimensional axisymmetric calculations.

4. Post-Experiment Analysis

In this section we present some simulations which help us understand the experiment discussed above. We will demonstrate that the experiment is an evolutionary improvement of the concepts presented in Section 2, rather than a quantum leap.

Figure 10 compares the driving pressure at the impact side of the flier for the original stepped barrel concept shown in Figure 5 and for the experimental configuration. There are two important observations to make about this figure. First, the drive pressure pulse width for the experiment is almost 50% longer than that for the idealized case (approximately an additional one microsecond longer). Second, the peak pressure in the drive pulse has fallen to around 75 GPa. The overall widening of the pulse is a result of the combination of (seemingly) small design changes that we made for the experiment. The reduced pressure is the result of the different impactor configuration and the presence of the TPX buffer. This has a major effect on the residual temperature of the flier. While this temperature was borderline melting in the idealized case, for the experimental case the temperature is estimated to be around 900 K, over a 50% reduction. The experimental flier is thus not close to melting. Because of the different drive properties, the estimated tensile states formed in the flier during launch are also different in the two cases. We estimate that the tensile states in the experimental flier are a little higher than for the idealization (48 kbars as opposed to 40 kbars).

We have performed a series of calculations that retrace the path that we explained in Section 2, but more closely related to the experimental configuration. Each calculation uses an impact velocity of 5.8 km/s. Calculation #1 is a 1-D Cartesian geometry calculation, in which no edge effects will be computed. All of the axial layers shown in Figure 7 are present in this calculation, with the same thicknesses. Calculation #2 is almost identical to calculation #1, except that it is a 2-D calculation in which a barrel has been placed and the layers have finite radial extent. The presence of the barrel contributes edge effects which were missing in #1. Neither calculation #1 nor calculation #2 can actually be replicated experimentally, because the impactor violates two-stage gun weight constraints. Calculation #3 introduces the impactor configuration of the experiment and a flier guard ring. The central flier has dimensions identical to that

in the experiment, but no stepped barrel is used. An experiment based on this calculation could be performed if so desired.

The predicted performance data for these calculations are given in Table 2. We compare the predicted axial velocities of these calculations with the exact experimental simulation in Figure 11. Perhaps the most interesting comparison is of the experiment simulation with the 1-D simulation, #1. The 1-D calculation under predicts the experiment simulation by over 8%. This is clear proof that edge effects are contributing in a positive manner to the flier terminal velocity. But, the full complexity of the stepped barrel is required to successfully exploit them. When we simply modify #1 to #2, so that lateral edge effects from a barrel participate during the launch process, the predicted velocity falls by an additional 9% from the 1-D calculation. Thus, without a stepped barrel the edge effects contribute to significant momentum loss in the launch.

We performed calculation #3 to account for the fact that the impactor in #1 and #2 could not be launched to 5.8 km/s in a real experiment. This problem is solved by the actual experimental configuration of the impactor and flier. Yet the predicted velocity of the flier *still falls further*, to 6.0 km/s. This calculation is quite similar to the first conceptual calculation discussed in Section 2, except for the more complex impactor configuration (six layers, as opposed to four), slight geometry differences in the flier/guard ring configuration, and the TPX buffer.

The introduction of the stepped barrel is the most important design feature. It results in flier velocities of 9.6 km/s, a 6% error with respect to the experimental value of 10.2 km/s. This error does not result from an inaccuracy in the estimate of the experimental impactor velocity. We performed an additional calculation of the experiment in which the impactor velocity was assumed to be 6.0 km/s. The predicted flier velocity was then 9.8 km/s, which is still in error by 4%. We have not explained the under prediction of the flier velocity in the calculations at this time.

The use of the TPX buffer on the flier is important. It provides an essential impact cushion for the flier, and is responsible for significantly lower temperatures in the flier than would be present without it. We simulated the experiment without that layer of low impedance material, and found that the flier melted (Chhabildas, *et al*, 1994b).

We demonstrate uniformity of the flier in the experiment simulation by plotting the axial velocity of the flier as a function of time at different radii near the impact side of the flier in Figure 12. The radius of 0.25-0.3 demarcates the central flier from the surrounding guard ring. The velocity uniformity through the main body of the flier is thus predicted to be exceptionally uniform. This is a critical condition for intact launch.

The long duration of the acceleration of the chunk is not simply a scaling result due to the increased thicknesses of the impactor and the flier. The early acceleration is influenced by wave reverberations and impedance considerations similar to the case of thin flier launch. However, late time acceleration of the central flier is dominated by multi-dimensional effects. These effects are primarily (1) the flow of the impactor material down the barrel, maintaining long time acceleration of the flier, and (2) coupling of the barrel extension to the system.

Layered impactor jetting down the barrel extension is important for launching the chunk. The layered impactor functions as a working fluid in this experiment when coupled with the use of a stepped barrel. It is important to tune

the impactor design so as to maximize forward momentum and kinetic energy transfer from the impactor to the chunk. The stepped barrel design and dimensional details of the impactor produce continued acceleration of the impactor materials following the impact. The length of time that acceleration occurs in the experiment shows how effective our current design is at achieving this effect.

A cautionary remark is that the equation of state descriptions of the impactor materials under cyclic loading (especially the TPX) become more important for accurately modeling this jetting. For this reason TPX is one material in particular that we are concerned about using the Mie-Grüneisen equation of state to describe. As the intensity of the loading of the TPX increases, it will tend to decompose, possibly accompanied by energy release. This phenomenon can not be modeled using a simple material description like the Mie-Grüneisen equation of state. Decomposition may indeed be occurring in the present experiment and our failure to model this process could be one reason that the **CTH** velocity predictions are smaller than the experimental velocities. However, even if decomposition takes place its effects are (apparently) small in the present experiment. In experiments involving different geometric configurations the influence of decomposition might be greater.

In Figures 13 and 14, axial material velocity for the experiment simulation is plotted as a function of axial distance on the axis of symmetry, at the times of 2.0 and 3.0 μs. Between these two times, the mean axial velocity of the central flier changes from 5.5 km/s (which is below the impact velocity of 5.8 km/s) to 8.6 km/s (which is well above the impact velocity). This is because materials in the layered portion of the impactor have begun to accelerate within the narrowed barrel of the experiment, causing additional acceleration of the central flier. At later times (not shown), we see further increase of the velocity of these materials, with some portions of the impactor achieving on-axis velocities of over 10 km/s, so that they are moving faster than the flier in the calculation at these times. The result of this is to maintain an efficient drive on the chunk. The continued drive contributes to the late time flier acceleration as seen in Figure 11.

It is very important to properly design the barrel extension. There are three different factors that play a role. The barrel must be stepped down to enhance impactor momentum and kinetic energy transfer to the central flier. This means that the downstream barrel diameter is an important parameter. The barrel extension must "inertially confine" the impact point so that severe deformation of the chunk does not occur. This causes a combination of factors related to barrel equation of state and the impactor configuration to become important. Finally, high pressure waves in the barrel resulting from the impact should not outrun the motion of the central flier. Otherwise, the barrel will squeeze the chunk too much, reducing its velocity and, more significantly, possibly fracturing it. This is also influenced by the barrel equation of state. It may not be possible to satisfy all of these constraints and it is not yet clear what the optimal design that best accounts for these constraints may be. One trade-off, for example, is that we require simultaneously high impedance barrels for inertial confinement and low sound speed barrels to slow down the pressure wave propagation ahead of the flier. An optimal material might therefore be depleted uranium, which has a higher density than the tungsten alloy we currently use, but a lower sound speed. This limits the choice of barrel materials. One advantage of the titanium alloy that we have used for the flier is that it has high ductility, along with a large fracture strength. Thus, our flier is fairly forgiving as to the region of barrel design parameter space that we focus on. As the technology is pushed to the limit, however, we would expect that every parameter will become important.

We have observed that at 2.0 μs the impact generated pressure waves are downstream of the flier in the barrel for the experiment. Prior to the experiment we could not be certain as to how sensitive the accelerator process was to these downstream compressive waves. The success of the experiment suggests that early time leading of the chunk by these waves is not detrimental to chunk integrity, our first experimental confirmation of this hypothesis. By 4.0 μs, however, the central flier has drawn even with the compressive barrel waves, and eventually will outrun them. Exactly the opposite of this effect occurred when the TPX buffer is removed. Very strong compressive waves in the barrel lead the chunk, resulting in strong pinching and ultimate break-up of the chunk during acceleration. This is an additional reason for having a TPX buffer: it covers the impact side of the stepped barrel, and decreases the amplitude of the compressive waves transmitted down the barrel.

While pressure confinement of the chunk is desirable, this may also contribute to the fracture of the chunk if it lasts too long or is too large. The impedance of the impactor is designed to prevent the type of loading that would cause the chunk to spall - *i. e.* fracture due to impact generated wave propagation effects. Just the right balance of parameters must be achieved in order to keep the flier intact while it is accelerated to high velocity. As indicated by the experimental radiographs in Figure 8, both of these goals seem to have been accomplished in this experiment, resulting in the launch of an intact chunk.

There is one further fact that demonstrates the working fluid behavior of the impactor. When the impact velocity was increased to 6.0 km/s, the flier residual temperature became smaller, as well as the tensile stress, while the velocity of the flier increased. The higher impact velocity produced greater heating, hence more vaporization, in the TPX. In the ANEOS Mie-Grüneisen model for TPX, an ad hoc method is used to represent expanded states. This model does not include the decomposition behavior mentioned earlier and is not guaranteed to provide an accurate vapor equation of state for this material. However, this equation of state is adequate for noting trends due to vaporization. Vaporization changes the compressibility, and so the cushioning effect, of the impactor and buffer, and causes lower pressures in the flier. At the same time, higher sound speeds of the compressed TPX produced higher expansion velocities, which were a little more successful at accelerating the flier. One should not expect this trend to continue for ever increasing velocities. At some point, the timing of the wave propagation will change sufficiently that a strong shock will enter the chunk, producing higher heating and spall formation.

Table 2 shows that we may have been quite close to fracturing the chunk in the experiment. The experiment simulation predicted approximately 5 GPa of tension in the middle of the chunk, which is comparable to the approximately 5.5 GPa spall strength of Ti6 alloy (Chhabildas, *et al*, 1990b). Note that the chunk in the experiment could have undergone an internal fracture that would not be visible to the experimental diagnostics. Spall strength tends to increase with strain rate (not modeled in our calculations) and under isentropic loading (Chhabildas and Asay, 1992). Hence, it is conceivable that under a structured time-dependent loading condition the material can sustain higher spall stresses than the nominal 5.5 Gpa.

5. Closure

This paper discussed the rational use of multi-dimensional calculations for designing hypervelocity launchers and analyzing the results of experiments. The current capabilities of computer hardware and software allow multi-dimensional shock wave calculations that predict reasonably accurate qualitative and quantitative trends for these complex experimental designs, and thus should be of interest to people developing advanced concepts in this field.

We oriented our discussion to the problem of the hypervelocity launch of an approximately unit aspect ratio flier. A series of conceptual calculations revealed that a primary component of the launch of such a flier is the use of a stepped barrel design. By studying a core design suggested by our calculations, an experiment was formulated that launched a 0.5 aspect ratio titanium alloy flier to a velocity of approximately 10.2 km/s the first time it was performed. The best numerical simulation of the experiment under predicts the flier velocity by 6%.

Key features of the experimental design that were identified by our computational analysis include:

- The experimental design incorporates 2-D effects in the impact region, while minimizing 2-D effects in the body of the chunk.
- The impactor design allows the impactor to function as a working fluid. This both cushions the flier, and maximizes momentum and kinetic energy transfer from the impactor to the chunk.
- The barrel extension design is different than the barrel extensions previously used for thin fliers. The barrel extension acts like an acceleration reservoir and contributes to the momentum and kinetic energy transfer efficiency while helping to minimize destructive 2-D effects in the chunk.

While we have not strictly identified the cause of the small under prediction of the experimental flier velocity, the problem may lie in our inaccurate equation of state for the TPX. The layered impactor materials are subjected to cyclic loading due to wave reverberations during the impact. A material like TPX may be particularly sensitive to this type of loading. Under these loads, the TPX tends to decompose, perhaps even accompanied by some energy release. Equations of state such as Mie-Grüneisen are not suitable for modeling the thermal behavior of low-density materials (TPX is 0.835 g/cc) under these loads. The resulting expansion velocity of decomposed TPX and other impactor materials may not be accurately modeled. This may incorrectly simulate the late-time drive on the flier induced by the jetting impactor. A more precise investigation would model the TPX with a more fundamental equation of state, such as a global SESAME table (Kerley, 1991). This approach could also model possible energy release from decomposition of the TPX.

It is interesting to examine the results in Figure 15. There, we have plotted axial momentum of the central flier as a function of time. This plot shows that the momentum conversion efficiency of this system is exceptionally small. The forward momentum of the impactor is approximately 165 kg-m/s. The final momentum of the flier is 3.1 kg-m/s. This represents a impactor-to-flier momentum conversion efficiency of 2%. Define the ***limiting momentum*** of the flier to be that momentum which it is possible to attain in planar impact driven systems where the impact velocity is 5.8 km/s. This value corresponds to the momentum when the central flier is moving at the velocity of 11.6 km/s (the limiting value of the flier velocity for planar impacts at 5.8 is double this velocity when an infinite mass impactor is used). In

the case of momentum, the central flier is within 18% of this limiting momentum. This result supports the hypothesis that achieving approximately unit aspect ratio flier velocities near 14.0 km/s, which exceeds the limit which is possible with non-complex impact techniques and which is a long-term objective of this project, will require greater impactor velocities and more precisely designed experimental configurations. It should be noted that a very small increase in the present momentum conversion efficiency between the impactor and the chunk, however, could result in a significant increase in the terminal velocity of the chunk. For example, an increase of the conversion efficiency to 4% would be more than sufficient.

REFERENCES

1. Barker, L. M. (1984), "High-Pressure Quasi-Isentropic Impact Experiments", in Shock Waves in Condensed Matter - 1983, Edited by J. R. Asay, R. A. Graham, and G. K. Straub, Elsevier Science Publishers, 217.
2. R. M. Brannon and L. C. Chhabildas (1994), "Experimental & Numerical Investigation of Shock-Induced Full Vaporization in Zinc", this conference.
3. Chhabildas, L. C. (1992), "Hypervelocity Launch Capabilities to over 10 km/s" in Recent Trends in High Pressure Research, 739.
4. Chhabildas, L. C., and J. R. Asay (1992), "Dynamic Yield Strength and Spall Strength Measurements Under Quasi-Isentropic Loading," in Shock Wave and High Strain-Rate Phenomena in Materials -1990 ed. by M. A. Meyers, L. E. Murr, K. P. Staudhammer, Marcel Dekker Inc., 947.
5. Chhabildas, L. C., J. R. Asay, and L. M. Barker (1988), "Shear Strength of Tungsten Under Shock- and Quasi-Isentropic Loading to 250 GPa", Sandia National Laboratories Report No. SAND88-0306.
6. Chhabildas, L. C., and L. M. Barker (1988), "Dynamic Quasi-Isentropic Compression of Tungsten", in Shock Waves in Condensed Matter - 1987, Edited by S. C. Schmidt and N. C. Holmes, Elsevier Science Publishers B. V., 111.
7. Chhabildas, L. C., L. M. Barker, J. R. Asay, and T. G. Trucano (1990a), "Relationship of Fragment Size to Normalized Spall Strength for Materials," J. Impact Engng., 10, 107-124.
8. Chhabildas, L. C., L. M. Barker, T. G. Trucano, and J. R. Asay (1990b), "Spall Strength Measurements on Shock-Loaded Refractory Materials," in Shock Waves in Condensed Matter - 1989, ed. by S. C. Schmidt, J. N. Johnson, and L. W. Davison, Elsevier Science Publisher, 429.
9. Chhabildas, L. C., L. M. Barker, J. R. Asay, T. G. Trucano, and G. I. Kerley (1991), "Sandia's New HyperVelocity Launcher - HVL," Sandia National Laboratories Report SAND91-0657.
10. Chhabildas, L. C., L. M. Barker, J. R. Asay, T. G. Trucano, G. I. Kerley and J. E. Dunn (1992), "Launch Capabilities to Over 10 km/s," in Shock Waves in Condensed Matter - 1991, Eds. S. C. Schmidt, J. Forbes. R. Dick, Elsevier Science Publishers B. V., 1025.
11. Chhabildas, L. C., J. E. Dunn, W. D. Reinhart, and J. M. Miller (1993a), "An Impact Technique to Accelerate Flier Plates to Velocities over 12 km/s" J. Impact Engng., 14, 121-132.
12. Chhabildas, L. C., E. S Hertel, and S. A. Hill (1993b), "Hypervelocity Impact Tests and Simulations of Single Whipple Bumper Shield Concepts at 10 km/s", Int. J. Impact Engng.; Vol. 14, 133-144.
13. Chhabildas, L. C., W. D. Reinhart, C. A. Hall, and L. N. Kmetyk (1994), "Launch Capabilities to 16 km/s," Sandia National Laboratories Report, SAND94-1272, 1994.
14. Chhabildas, L. C., T. G. Trucano, W. D. Reinhart, and C. A. Hall (1994), "'Chunk' Projectile Launch Using the Sandia Hypervelocity Launcher Facility," Sandia National Laboratories Report, SAND94-1273, 1994.
15. E. S. Hertel (1992), "The CTH Data Interface for Equation-of-state and Constitutive Models," Sandia National Laboratories, SAND92-1297.

16. Kerley, G. I. (1991), "CTH Reference Manual: The Equation of State Package,", Sandia National Laboratories Report SAND91-0344.

17. McGlaun, J. M., S. L. Thompson, and M. G. Elrick (1990), "CTH: A Three-Dimensional Shock-Wave Physics Code," Int. J. Impact. Engng.; Vol. 10, 351-360.

18. Thompson, S. L. (1989), "ANEOS Analytic Equations of State for Shock Physics Codes Input Manual," Sandia National Laboratories, SAND89-2951.

Table 1: Important computational parameters related to the requirement for a stepped barrel extension.

Calculation Description	Maximum Pressure at Impact Side of Flier (kbars)	Flier Velocity (km/s)	Estimated Tensile Pressure (GPa)	Residual Flier Temperature (K)	Flier Intact?
Titanium guard ring - no step	85	6.0	> 5	1200	Maybe
Tungsten guard ring - no step	104	7.0	>> 5	1500	No
Tungsten guard ring - stepped barrel	105	> 10	4	1000 - 2000	Maybe

Table 2: Performance data from CTH calculations related to the experiment. The flier velocity error is measured with respect to the measured experimental velocity of 10.2 km/s.

Calculation.	Chunk Velocity (km/s)	Predicted Velocity Error (%)	Maximum Driving Pressure (GPa)	Maximum Tensile Pressure (GPa)	Residual Temperature (K)
Experiment	9.6	6	75	4.8	900
#1	8.8	15	65	< 0.5	850
#2	8.0	23	65	2.1	725
#3	6.0	41	70	> 4.7	850

DISCLAIMER

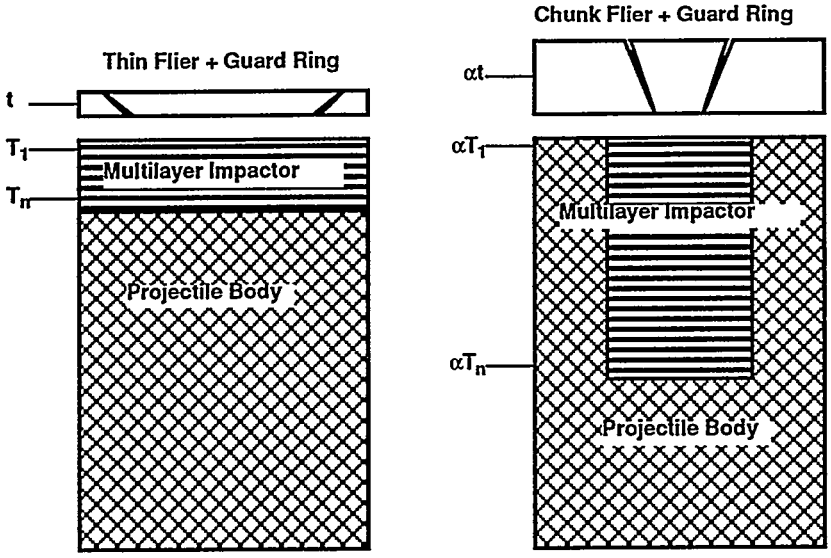

Figure 1. The change in multilayer configuration when passing from the thin flier to the chunk flier. The thickness t of the original thin flier has increased by a factor of α. The multilayer, consisting of n variable impedance layers of thicknesses T_n, then nominally increases in thickness by the same factor α. To remain within the weight constraint of the two-stage gas gun projectile, the diameter of the multilayer must decrease. The separation between the guard ring and the flier is exaggerated in this figure.

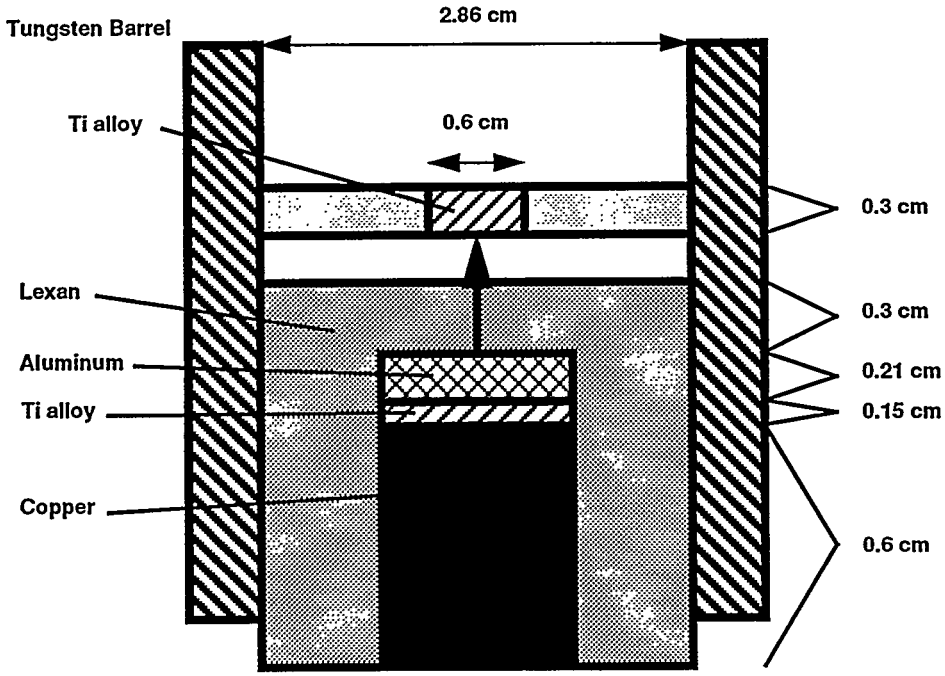

Figure 2. An idealized impactor for studying barrel extension concepts. The impactor is shown in a barrel configuration in which there is no stepped barrel. The drawing is not to scale.

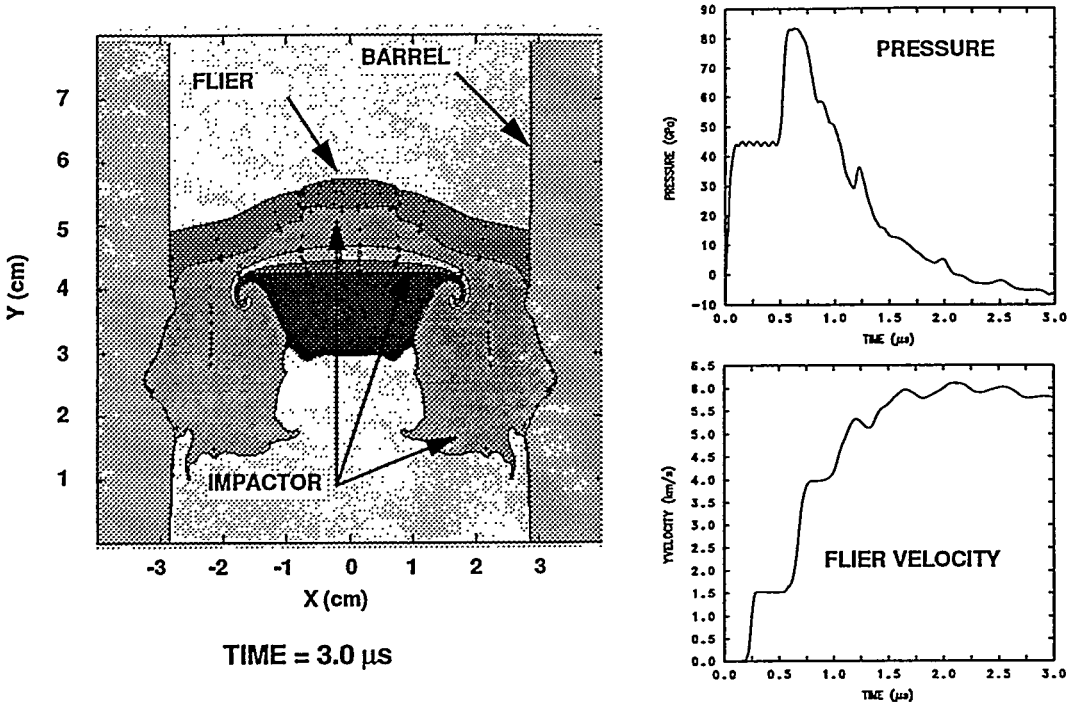

Figure 3. The simulated configuration of the impact launch of a titanium flier at 3.0 microseconds. We have also shown the loading pressure generated by the simplified graded density impactor and the velocity history of the flier. The calculated terminal velocity of the chunk in this case is ~ 6 km/s, for an impact velocity of 5.8 km/s.

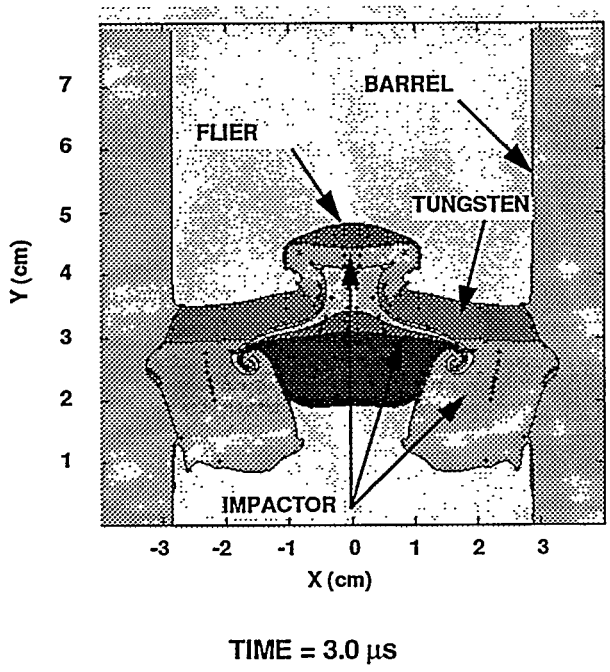

Figure 4. The simulated configuration of the impact launch of a titanium flier at 3.0 microseconds with a tungsten guard ring. The flier is moving faster, and is far more distorted, than the equivalent time in Figure 3 with a titanium flier.

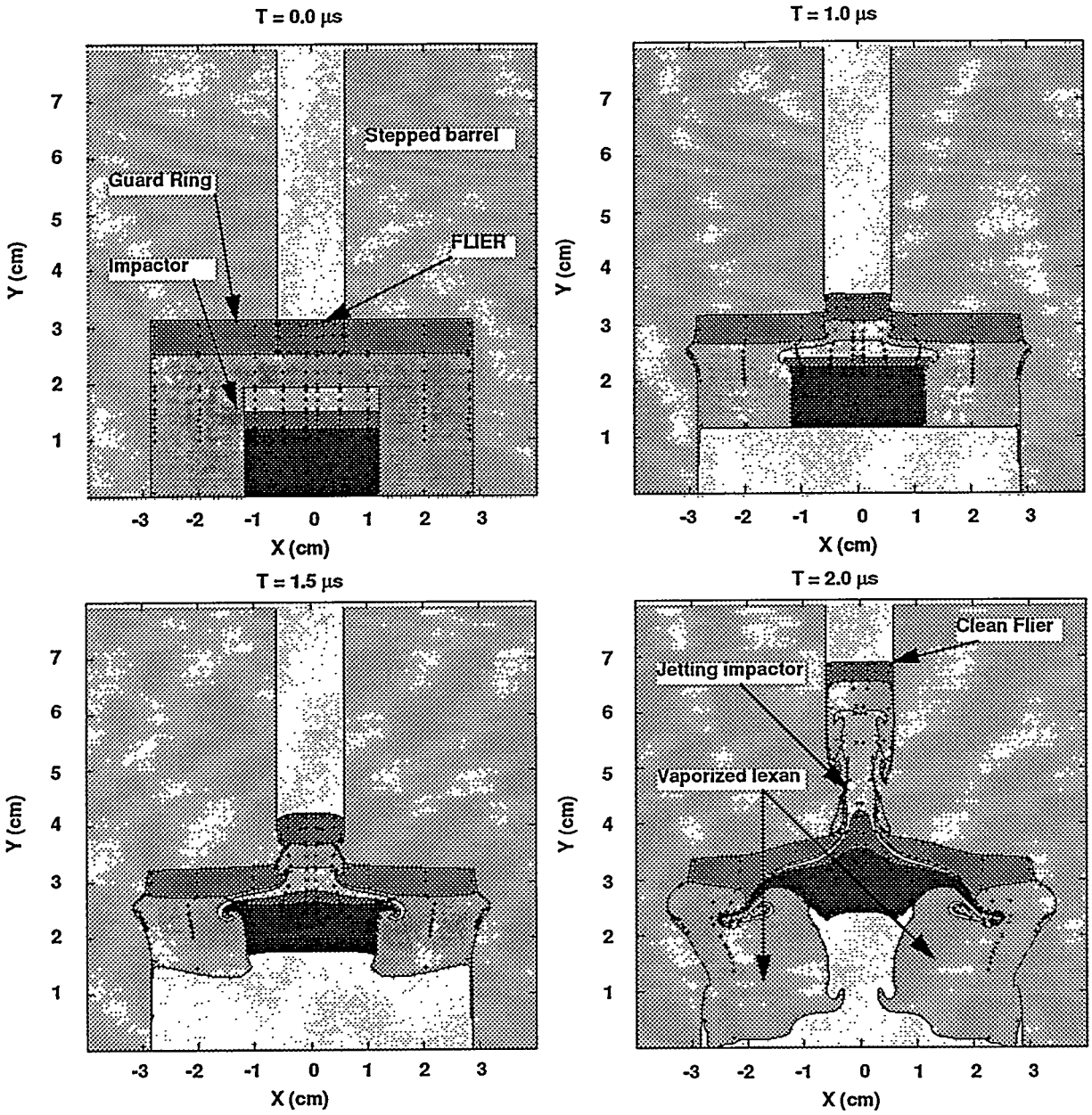

Figure 5. CTH simulation of a chunky flier launch using a stepped barrel. The impactor velocity is 5.8 km/s. The flier is titanium alloy and the guard ring is tungsten alloy. At 3.0 microseconds velocity of the flier is greater than 10 km/s.

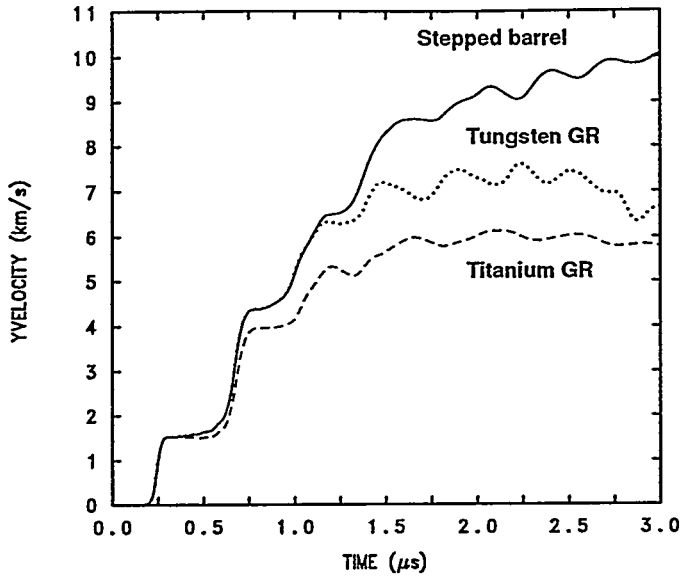

Figure 6. Axial velocity of the titanium chunk flier as a function of time plotted for three different CTH calculations: (1) titanium guard ring (GR) without a stepped barrel; (2) tungsten guard ring without a stepped barrel; and (3) tungsten guard ring with a stepped barrel. The velocity is measured at a location at the center of the flier.

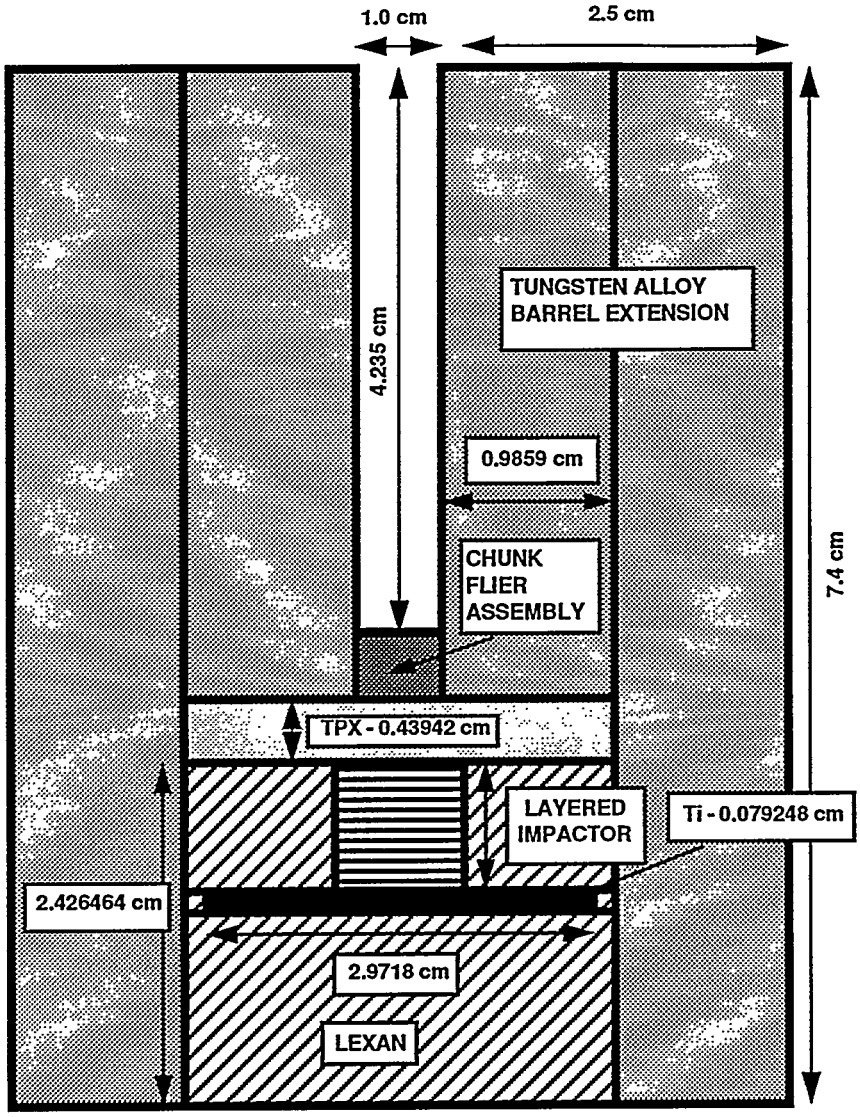

Figure 7. Schematic of the experimental configuration. The major differences in this configuration from the simplified stepped barrel configuration discussed in Section 2 are: (1) The flier and its guard ring are inserted in the barrel extension, flush with a protective TPX cushion and (2) the impactor configuration has more layers to provide a better quasi-isentropic pressure drive. Both the guard ring and the central flier are accelerated by the impact. The drawing is not to scale.

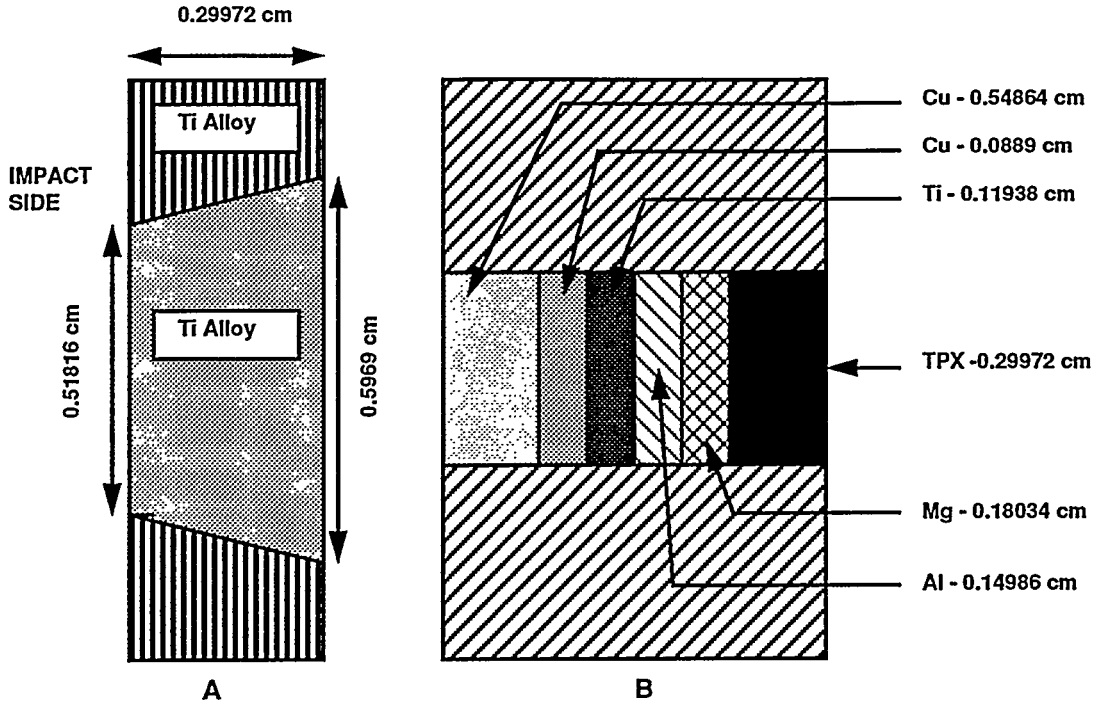

Figure 8. Schematic of the layered impactor and the flier plate/guard ring configuration. The drawings are not to scale.

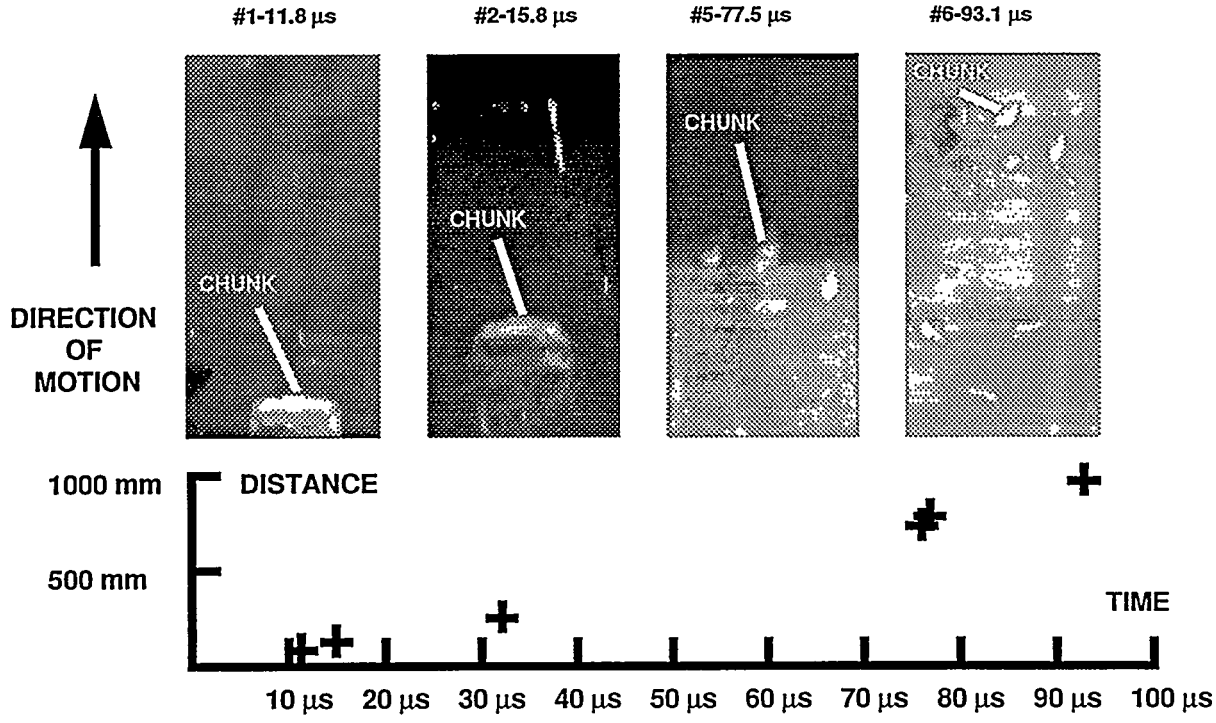

Figure 9. Schematic of the layered impactor and the flier plate/guard ring configuration. We have also plotted the measured positions and times for radiographs out to 100 μsec.

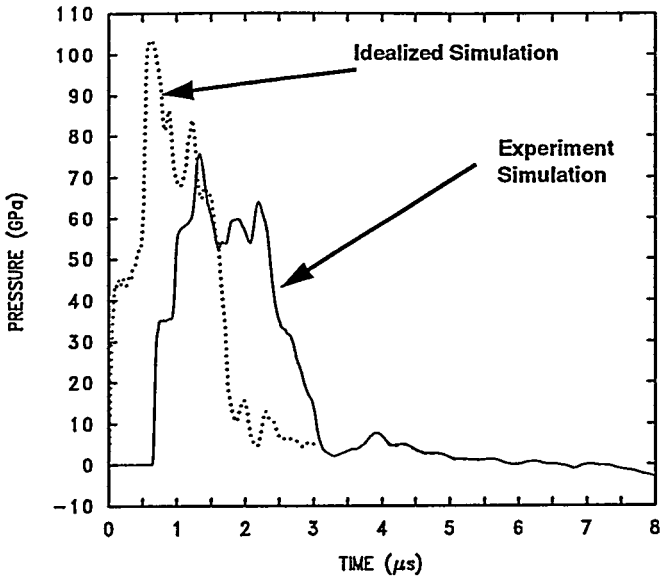

Figure 10. Comparison of the drive pressures for the idealized and the experimental configuration.

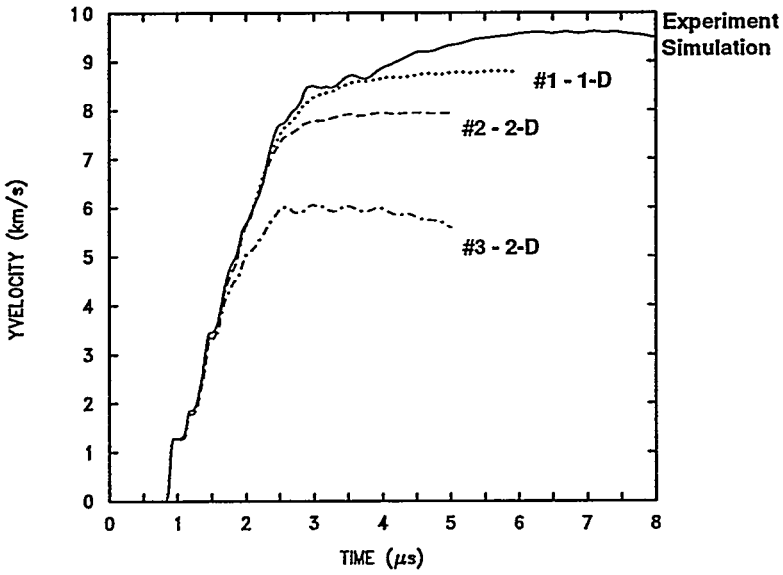

Figure 11. Comparison of the axial flier velocities for four different variations of the experimental configuration. The velocity is measured at the center of the flier.

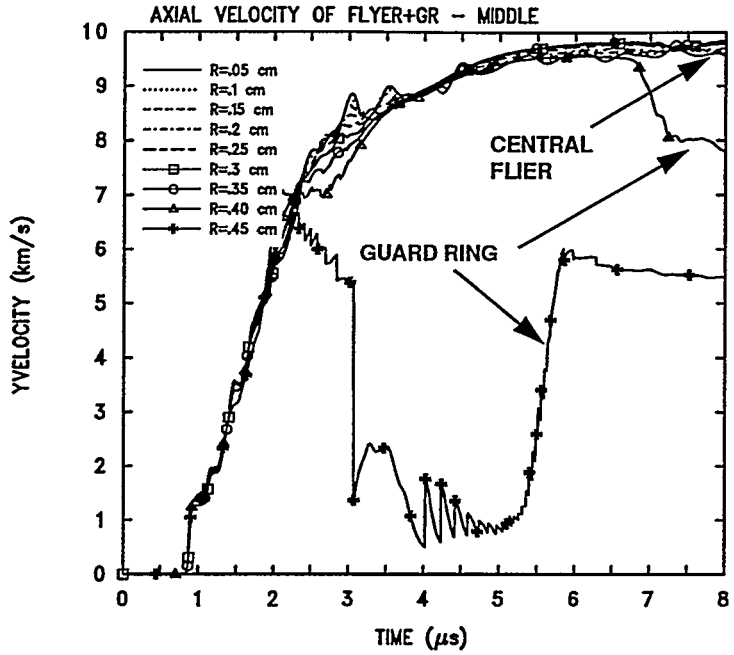

Figure 12. Axial velocity vs time at different radii near the impact side of the flier configuration. The inner radius of the guard ring at the impact side is approximately 0.25 cm. Material in the guard ring begins to deform badly as early as 2.0 microseconds. By 8.0 microseconds, part of the guard ring is actually moving slightly faster than the central flier. The nonuniformity of the velocities in the central flier is approximately 0.1 - 0.2 km/s.

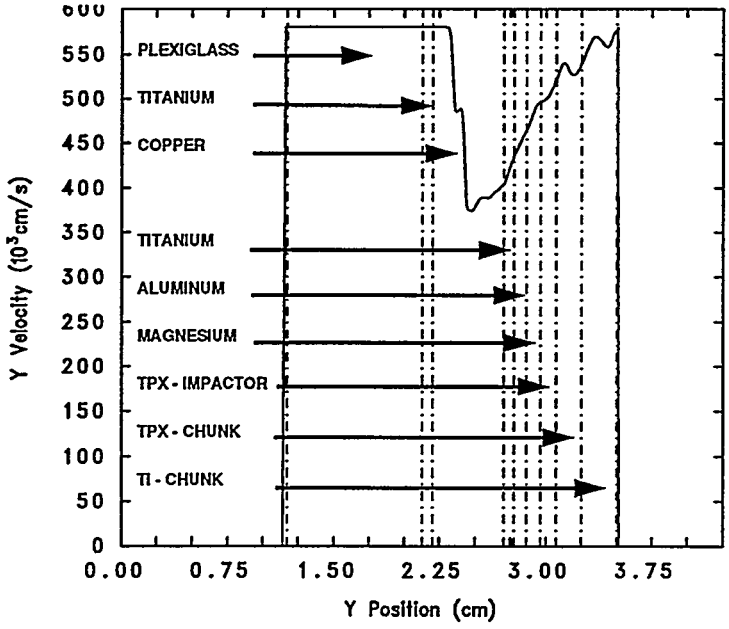

Figure 13. Axial velocity as a function of axial position at 2.0 μs and the corresponding system configuration from the CTH calculation of the experiment. The central flier is not yet moving faster than the initial impactor velocity.

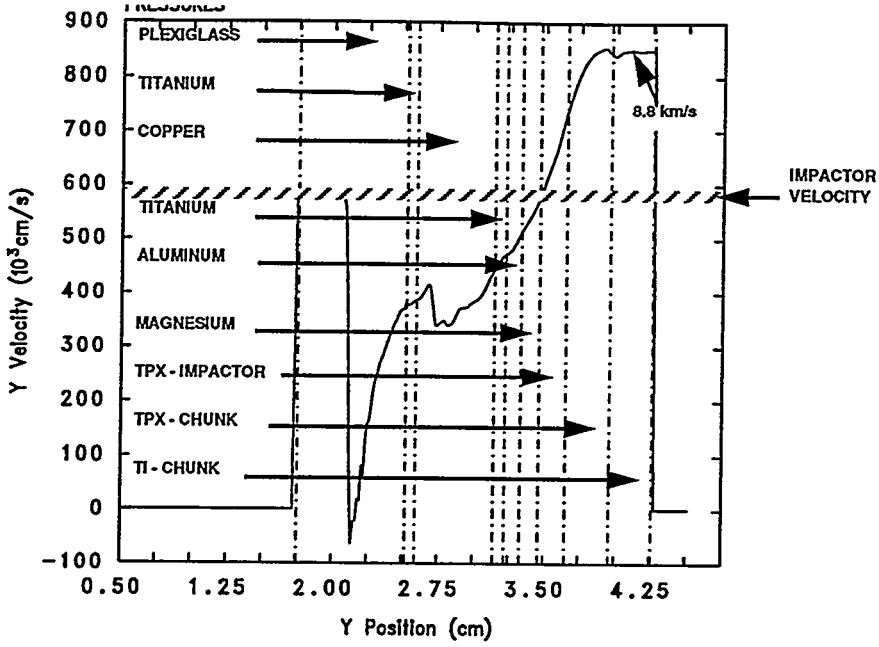

Figure 14. Axial velocity as a function of axial position at 3.0 μs on the axis of symmetry. The central flier is now moving faster than the initial impactor velocity. The TPX buffer and the TPX impactor layer both have a higher velocity than the impact velocity.

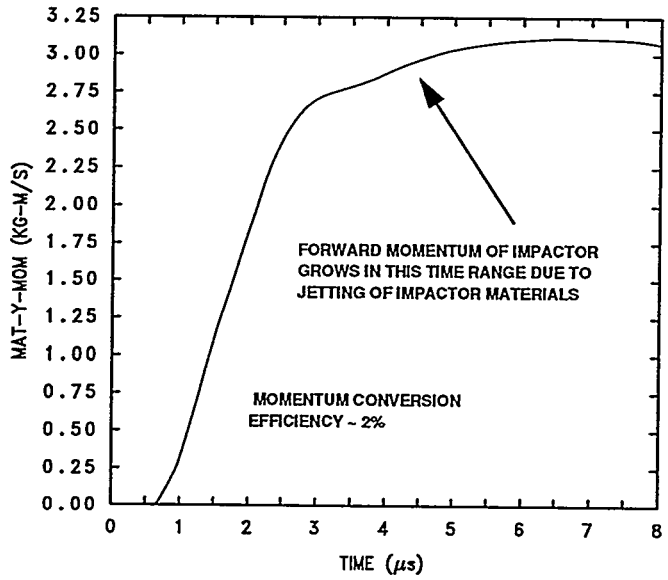

Figure 15. Momentum of the flier as a function of time in the experiment simulation.